Environment International 136 (2020) 105375

Contents lists available at ScienceDirect

Environment International

journal homepage: www.elsevier.com/locate/envint

Full length article

ReAFFIRM: Real-time Assessment of Flash Flood Impacts – a Regional high-resolution Method

Josias Ritter*, Marc Berenguer, Carles Corral, Shinju Park, Daniel Sempere-Torres

Center of Applied Research in Hydrometeorology, Universitat Politècnica de Catalunya, BarcelonaTech, Jordi Girona 1-3 (C4), 08034 Barcelona, Spain

ARTICLE INFO

Handling Editor: Zhen (Jason) He

Keywords:
Flash flood
Flood impact modeling
Real-time impact assessment
Early warning system
Uncertainty
Flood risk management

ABSTRACT

Flash floods evolve rapidly in time, which poses particular challenges to emergency managers. One way to support decision-making is to complement models that estimate the flash flood hazard (e.g. discharge or return period) with tools that directly translate the hazard into the expected socio-economic impacts. This paper presents a method named ReAFFIRM that uses gridded rainfall estimates to assess in real time the flash flood hazard and translate it into the corresponding impacts. In contrast to other studies that mainly focus on individual river catchments, the approach allows for monitoring entire regions at high resolution. The method consists of the following three components: (i) an already existing hazard module that processes the rainfall into values of exceeded return period in the drainage network, (ii) a flood map module that employs the flood maps created within the EU Floods Directive to convert the return periods into the expected flooded areas and flood depths, and (iii) an impact assessment module that combines the flood depths with several layers of socio-economic exposure and vulnerability. Impacts are estimated in three quantitative categories: population in the flooded area, economic losses, and affected critical infrastructures. The performance of ReAFFIRM is shown by applying it in the region of Catalonia (NE Spain) for three significant flash flood events. The results show that the method is capable of identifying areas where the flash floods caused the highest impacts, while some locations affected by less significant impacts were missed. In the locations where the flood extent corresponded to flood observations, the assessments of the population in the flooded area and affected critical infrastructures seemed to perform reasonably well, whereas the economic losses were systematically overestimated. The effects of different sources of uncertainty have been discussed: from the estimation of the hazard to its translation into impacts, which highly depends on the quality of the employed datasets, and in particular on the quality of the rainfall inputs and the comprehensiveness of the flood maps.

1. Introduction

Numerous flash floods (FF hereafter) occur across the globe every year. In Europe, a yearly average of around 50 FF-related fatalities is recorded (Sene, 2013). Apart from posing a high danger to humans, economic losses in the range of several billion euros can be caused by individual events (CRED, 2016; EEA, 2010; Gaume et al., 2009).

Typically, FFs occur in small to medium-sized catchments with steep slopes and prone to convective storms. This setting results in very short lag times between the causative rainfall and the discharge response in the stream channel – usually not more than a few hours (Georgakakos, 1986; Hapuarachchi et al., 2011). This extremely sudden onset is one of the main drivers for the devastating potential of FFs (EEA, 2010; Sene, 2013; Spitalar et al., 2014) since it leaves only little time to coordinate flood response measures (e.g. evacuations or installations of non-permanent flood protection systems).

Early warning systems (EWS) can help to extend the anticipation horizon of FFs; the European Environmental Agency (EEA, 2010) argues that the improvement of EWSs is the most effective measure to reduce FF impacts. One way to improve EWSs is to increase the forecast skill (e.g. by improved rainfall estimation and forecasting). Another way is to include additional information into the EWS to enhance the decision support for the emergency responders (e.g. by simulating the response to the rainfall in the stream network). The latter was the motivation of several methods that forecast the FF hazard (e.g. the return period or discharge at predefined river sections; see Alfieri et al., 2019, 2012; Corral et al., 2019; Gourley et al., 2014; Hapuarachchi et al., 2011 for reviews).

Many of these studies used radar data as the source for the quantitative precipitation estimation (QPE). Although the radar provides rainfall estimates from indirect observations and thus it has limitations in terms of

* Corresponding author.
E-mail address: ritter@crahi.upc.edu (J. Ritter).

https://doi.org/10.1016/j.envint.2019.105375
Received 21 June 2019; Received in revised form 6 November 2019; Accepted 28 November 2019

accuracy, the very high temporal and spatial resolutions of the radar measurements depict the high variability of convective storms that are often the cause for FFs (Alfieri et al., 2012). Moreover, the radar QPE can be extrapolated to forecast rainfall for the coming few hours (nowcasting) with a higher accuracy than numerical weather prediction models (Berenguer et al., 2012). There is great potential in combining radar nowcasting with hydrological models (for a review see Berne and Krajewski, 2013). In the context of FFs, this idea was adopted in several studies to forecast discharge at a given location of interest (e.g. Berenguer et al., 2005; Blöschl et al., 2008; Javelle et al., 2014; Silvestro and Rebora, 2011) and trigger FF warnings. In monitored catchments, hydrological models can be calibrated to simulate the runoff behaviour well. In ungauged catchments (as often the case in areas prone to FFs), this calibration can only be done by parameter transfer from similar or parent catchments (e.g. Norbiato et al., 2008), or with simplified models of estimating initial conditions, such as soil moisture accounting schemes (Javelle et al., 2010; Raynaud et al., 2015).

The probably most prominent example of such hydrologically-based FF warning systems is the widely used Flash Flood Guidance method (FFG), which has been running operationally in the USA since the 1980s (Clark et al., 2014; Georgakakos, 2006, 1986). This method triggers a warning for a given catchment when the forecasted rainfall exceeds the threshold that produces bankfull discharge at the catchment outlet. The threshold is dynamically updated depending on the initial conditions of the catchment, such as the soil moisture content.

An alternative way to generate FF warnings is to directly compare rainfall (both observed and forecasted) to fixed intensity-duration thresholds, without employing a full hydrological model; see Alfieri et al. (2019) for some examples. These methods do not require information on initial conditions and parameter calibration for individual catchments, and computation times are short. This makes these rainfall-based approaches attractive for real-time application over larger spatial domains. According to the GRADEX method, derived by Guillot and Duband (1967) from the analysis of long-term records of rainfall and discharge in France, the initial catchment conditions can be important for events with return periods below 10 years. For events with higher return periods, their impact on catchment response is generally smaller. Similar studies carried out by Wood et al. (1990) and Grillakis et al. (2016) supported this hypothesis, although Borga et al. (2007) and Marchi et al. (2010) found cases in which extremely dry or wet initial conditions played a significant role also during extreme flash floods.

An example of such a rainfall-based approach is the ERICHA system (European Rainfall-InduCed Hazard Assessment, originally named FF-EWS; see Alfieri et al., 2019; Corral et al., 2019; 2009). By comparing (observed and forecasted) rainfall to climatological thresholds of basin-aggregated rainfall, the ERICHA system assesses the hazard by means of the exceeded return period over the drainage network. It has been running operationally for several years at the Water Agency of Catalonia (NE Spain; Corral et al. 2009) and it has been recently updated and applied at higher resolution in several regions in Europe in the context of the H2020 project ANYWHERE. The same system was also applied in the context of the ERICHA project to qualitatively estimate the FF hazard level at European scale (Park et al., 2019) and it has been running operationally in the European Flood Awareness System (EFAS) since 2017.

All of the previously mentioned approaches predict the hydro-meteorological FF phenomenon in pure hazard terms (e.g. the peak discharge or the return period). As a base for organising flood response measures, the resulting socio-economic consequences need to be estimated, and this can be done by combining the hazard forecast with information about exposure and vulnerability of the area at risk. In current practice, this is mostly done non-automatically by the emergency managers during the event occurrence, which poses two issues (WMO, 2015): Firstly, the non-automatic impact estimation highly depends on the individual knowledge and experience of the person in charge, which potentially results in subjective, suboptimal decisions; secondly, this process is time-consuming and reduces the temporal margin to coordinate flood response measures. This is particularly problematic during FFs when every minute counts and potentially determines if a warning reaches the responders in time or not. Therefore, the WMO (2015) suggests the development of complementary approaches that automatically predict the socio-economic impacts that result from the hazard, which can enable more effective and faster emergency responses.

Several promising approaches have been developed for forecasting flood impacts in large rivers (e.g. Aldridge et al., 2016; Cole et al., 2016; Revilla-Romero et al., 2017). The Rapid Flood Risk Assessment (Dottori et al., 2017) is running operationally in EFAS, covering all European rivers with a catchment area larger than 500 km^2. In the field of FFs, forecasting impacts in real time is more challenging, since the location and intensity of the triggering rainfall system might develop quickly. Existing methods mostly aim at estimating specific impacts (e.g. the number of flooded properties or the flooding of the road network) to improve the decision-making in individual river catchments or relatively small regions (e.g. Le Bihan et al., 2017; Saint-Martin et al., 2016; Silvestro et al., 2019; Vincendon et al., 2016). For authorities that act on larger scales, it can be useful to monitor impacts in entire regions or nations. Calianno et al. (2013) combined FFG hazard warnings with land use and population density maps to define and forecast qualitative impact levels in Oklahoma (USA). This represents a first benchmark for FF impact forecasting at regional scale.

This paper describes a novel method (ReAFFIRM) for real-time assessment of quantitative FF impacts at regional scale and high resolution. The method is designed to be integrated into an EWS to provide emergency managers with information on the expected flooded area and the resulting impacts. This is achieved by combining FF hazard outputs with flood maps and exposure and vulnerability datasets that are nowadays publicly available in many locations (e.g. throughout Europe).

The objective of this work is to evaluate the capacity of ReAFFIRM to identify FF impacts. With this aim, its performance has been studied in the region of Catalonia (NE Spain), covering an area of more than 32.000 km^2. ReAFFIRM has been run offline simulating real-time conditions, using post-processed radar QPE as input. Although ReAFFIRM is designed to be used for impact forecasting, this study evaluates the quality of the impact estimates (i.e. based on observed rainfall) to focus on the added value of the transformation of FF hazard into impacts.

All the elements involved in the assessment of FF impacts are subject to different sources of uncertainty. Several authors (Berenguer et al., 2011; Germann et al., 2009; Ntelekos et al., 2006; Yatheendradas et al., 2008; Zappa et al., 2010) discussed the underlying uncertainties of FF hazard assessment and forecasting. Among them, the errors in the rainfall estimation (and rainfall forecast) are quite significant and have a direct effect on the quality of FF hazard forecasts (Hapuarachchi et al., 2011). The translation from hazards into impacts introduces additional uncertainties, whose effect on the final impact estimates is often even higher (Jonkman, 2007; Merz et al., 2007); these are mostly related to the empirical nature of flood exposure and vulnerability data, such as depth-damage curves (de Moel and Aerts, 2011). To mitigate the risk of misinterpretation of forecasts by the end users, it is essential to analyse and communicate the existing sources of uncertainty (Faulkner et al., 2007; Ramos et al., 2013; WMO, 2008). Throughout this paper, the effects of some uncertainty sources affecting ReAFFIRM are discussed.

In Section 2, the individual components of ReAFFIRM are presented. The application and setup in the case study area of Catalonia (NE Spain) is described in Section 3. In Section 4, the simulation results for three significant FF events are compared to a variety of post-event impact evidences (including newspaper articles, insurance claim records, emergency calls, and social media postings), to analyse the performance of the overall system and identify uncertainties in the individual components. Finally, some conclusions on the capabilities and limitations of the method are drawn in Section 5.

2. Method

The goal of ReAFFIRM is to provide quantitative real-time

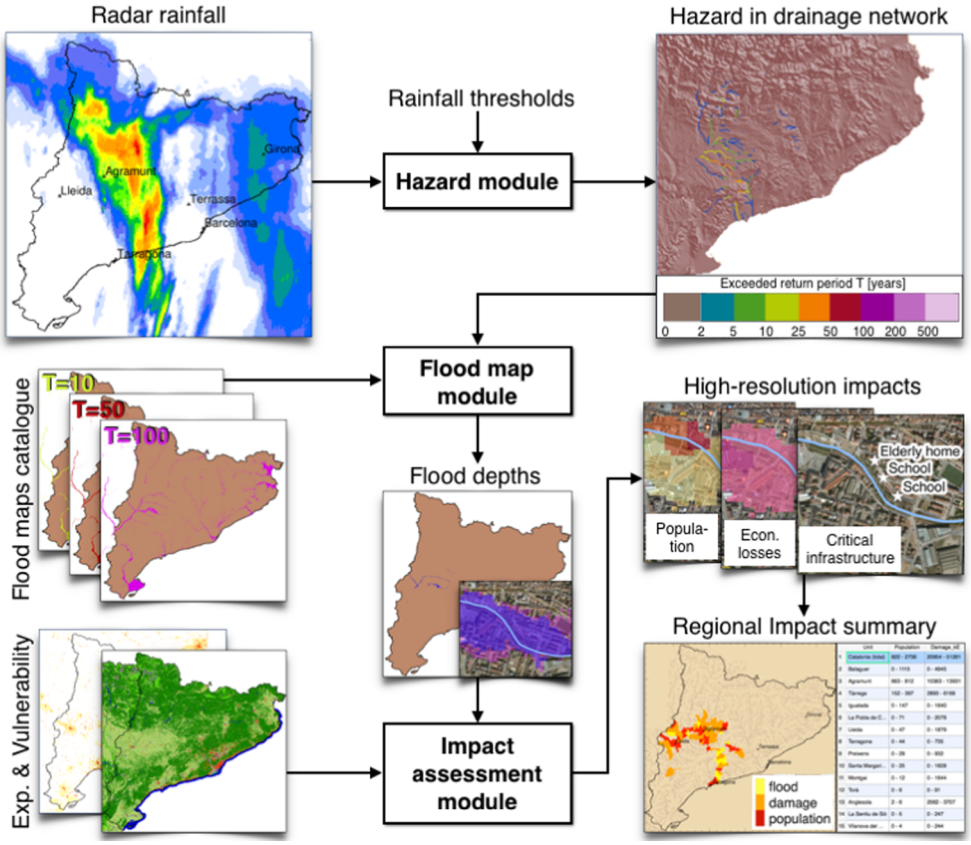

Fig. 1. Framework of the method ReAFFIRM that converts radar rainfall into FF impact assessments.

assessments of socio-economic FF impacts at regional scale. This is done by the following three main steps (Fig. 1): First, rainfall estimates are used as input to a FF hazard module that assesses the exceeded return period along a gridded drainage network. Then, a flood map module relates the return periods in the drainage network to high-resolution flood extents and depths. In the third step, an impact assessment module combines the high-resolution flood depths with socio-economic exposure and vulnerability information in the flooded area. The results are quantitative assessments of the population in the flooded area, economic losses, and affected critical infrastructure.

To ensure high practical value, the design of ReAFFIRM is subject to two constraints: i) applicability at regional scale, and ii) low computational cost to facilitate operation in real-time. To satisfy these constraints, two choices have been made: Firstly, for the hazard estimation, a rainfall-based approach has been selected, which ensures quick computation times (in contrast to complex hydrological models) and avoids the difficulty of calibrating parameters of numerous (often unmonitored) catchments. Secondly, for the estimation of the flood depths, a catalogue of pre-calculated flood maps has been employed, instead of doing hydraulic calculations in real-time, which is at regional scale computationally not feasible.

2.1. Flash flood hazard estimation – The ERICHA system (Corral et al., 2019)

ReAFFIRM uses the simulations of the ERICHA system to assess the FF hazard in the drainage network. The ERICHA system is rainfall-based and estimates the FF hazard in terms of the exceeded return period along the gridded drainage network, retrieved with a user-defined spatial resolution. The exceeded return period is computed at each stream cell by means of the rainfall averaged over the upstream drainage area (i.e. the basin-aggregated rainfall) and accumulated over a window equal to the concentration time of the upstream basin. The resulting basin-aggregated rainfall over this accumulation window is compared to basin-aggregated Intensity-Duration-Frequency (IDF) rainfall thresholds that are obtained from climatology. This comparison enables to determine the value of the exceeded return period in each cell of the drainage network. Fig. 2a shows an example of the resulting FF hazard output in a catchment.

2.2. Flood map module

The flood map module translates the exceeded return periods estimated by the ERICHA system into high-resolution flood extents and depths for the entire region. The base for this step is a catalogue of flood maps related to several return periods. Creating such a catalogue at regional scale, including also the small streams that are prone to FFs, is a tremendous amount of work out of the scope of this study. Instead, the already existing flood maps created by means of hydraulic modelling within the EU Floods Directive have been adopted; see European Commission (2015) for a summary of the methods used and the return periods available in each Member State). Each flood map from the catalogue contains flood depth values over a grid at very high resolution (typically 1–5 m). In ReAFFIRM, these maps have been upscaled to a coarser resolution (as a reference, 25 m) to be used in real time at regional scale. The resulting cells with an average flood depth exceeding 0 cm are referred to as “flood cells” in the following. Whereas the information about flood extents is freely accessible in all EU Member States, this is not always the case with the information on flood depths. In such cases, we have opted to assume a uniform value of flood depth.

The flood map module uses this catalogue as the base for translating the return period output of the ERICHA system into estimates of flood depths. With this aim, each of the high-resolution flood cells has been assigned to the nearest drainage network cell of the ERICHA system. In operation, the flood map module makes use of this assignment in the following way: If the ERICHA system identifies a significant value of exceeded return period in a given drainage network cell, all flood cells

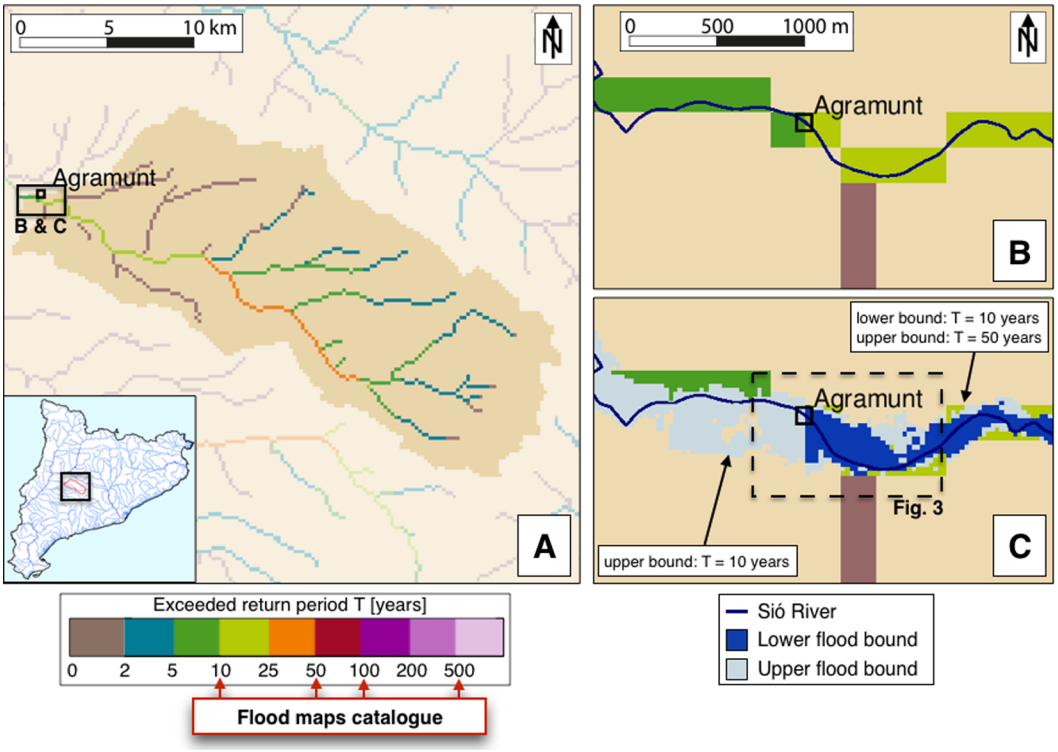

Fig. 2. (a) Example of the ERICHA FF hazard in the gridded drainage network of the Sió River upstream of Agramunt (Catalonia, NE Spain; 02.11.2015 1942 UTC) at a resolution of 200 m. (b) Zoom to the area of Agramunt. (c) Resulting output of the flood map module: lower and upper flood bounds in high resolution. For exceeded return periods of T = 5 years, no lower flood bound is computed.

that are assigned to this drainage network cell are activated, and the flood depth values are retrieved from the flood map of the corresponding return period.

Because the ERICHA system estimates the hazard in terms of exceeded (i.e. not exact) return period values, the flood depths of the corresponding return period represent the "lower bound". If the corresponding return period is not available in the catalogue, the flood depths of the next lower flood map are retrieved as the "lower bound". To compute an "upper bound", the flood depths of the next higher flood map in the catalogue are also retrieved. This is illustrated with an example of the input (Fig. 2b) and output (Fig. 2c) of the flood map module. For the drainage network cells with an exceeded return period value of T = 10 years, two flood maps are retrieved from the catalogue: the maps of T = 10 years (lower flood bound) and T = 50 years (upper flood bound, the next available return period in the catalogue of the given example, as indicated in the legend of Fig. 2a). Downstream of the town of Agramunt, the exceeded return period decreases to T = 5 years (Fig. 2b). Since the catalogue does not contain any flood map for return periods smaller than 10 years, only the upper flood bound (T = 10 years) is computed (Fig. 2c). For exceeded return periods smaller than 5 years, no flood maps are retrieved.

The resulting output of this module covers the entire region with two high-resolution grids (i.e. lower and upper flood bounds) containing values of flood depth along the river reaches that are included in the flood maps catalogue.

2.3. Impact assessment module

The impact assessment module translates the flood extents and depths estimated by the flood map module into quantitative assessments of socio-economic impacts. This is done based on an automatic combination of the flood depths with information about socio-economic exposure and vulnerability in the flooded area. It has been decided to separate the impacts into categories that can be expressed in quantitative terms. ReAFFIRM considers the following impact categories:

(i) Population in the flooded area: For emergency responders, an estimation of the number and distribution of population in the flooded area can be useful, for instance, to coordinate evacuations. In each flood cell, the population density value is retrieved from a population density map. The result is a map showing the distribution and density of population in the flooded area (see Fig. 3 for an example).

(ii) Economic losses: The economic losses are estimated by combining a) the simulated flood depths from the flood map module, b) a land use map, and c) depth-damage curves for all land use classes. The result is a map with loss values of € / m^2 within the flood extent.

(iii) Affected critical infrastructures: Critical infrastructures include particularly vulnerable elements (e.g. schools or hospitals), and elements that can cause so-called "cascading effects" – their failure exacerbates impacts elsewhere, e.g. transportation infrastructure or power plants (Association of State Floodplain Managers, 2011; Schauwecker et al., 2019). Indicating the potentially affected critical infrastructures during a FF can support the responders in the coordination of their actions (e.g. the activation of emergency and self-protection plans). The impact assessment module of ReAFFIRM employs a geo-referenced database of critical infrastructures to identify those that are within the simulated flood extent. Apart from the type and location of the affected critical infrastructure, potentially available details such as the contact phone number can be automatically provided to the responders.

The estimations of the three impact categories are done for both the lower and the upper flood bounds obtained with the flood map module, resulting in two high-resolution impact outputs in each of the three categories. The high-resolution flood extents and the impact outputs can be used to support emergency management decisions at the local level, such as closing specific roads or disseminate warnings to specific neighbourhoods. When monitoring impacts over an entire region, a summary of the identified impacts at the municipality level can be useful (in particular given the time constraints during FFs). Table 1 and

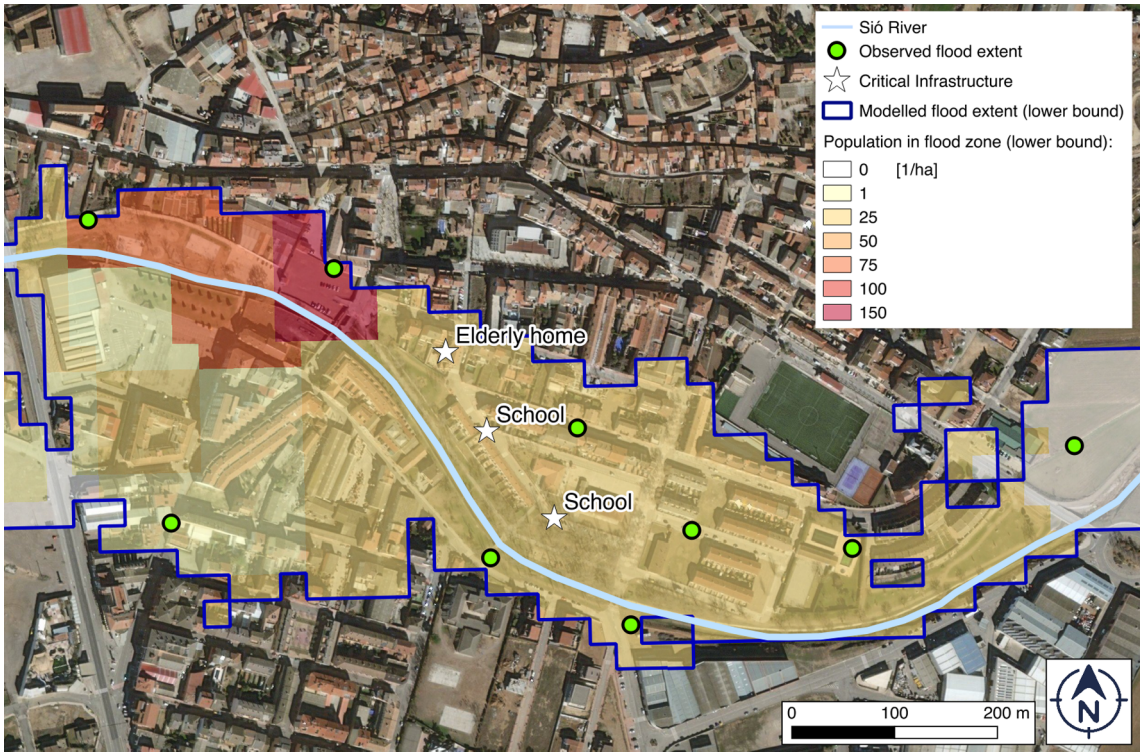

Fig. 3. Simulated population density in the flooded area (lower bound; 02.11.2015 2212 UTC) in Agramunt (Catalonia).

Fig. 4 (left panel) illustrate an example of the impact summary output at a particular moment during a FF (corresponding to the situation of Fig. 3). Table 1 provides the quantitative impact information of the lower and the upper bounds in each impact category (shown as ranges). For simplicity, the affected critical infrastructures are listed for the upper bound only. In Fig. 4, the summary maps show the impacts corresponding to the upper bound (safe side) and highlight the municipalities potentially affected by flooding.

To give an idea of the moderate computational requirements of the method: starting from the corrected QPE, the computation of hazards and impacts for the situation shown in the left panel of Fig. 4 took around 5 min on a standard server.

3. Case study area and data

ReAFFIRM has been applied in the region of Catalonia (NE Spain). This area is frequently affected by FFs, especially during the autumn months, when the high surface temperatures of the Mediterranean Sea favour the formation of warm and moist air masses. When these air masses reach the coastline, they encounter in many locations steep terrain that forces them upwards, often resulting in high rainfall intensities. The steep terrain slopes and the high degree of urbanisation provoke very quick discharge responses in the drainage network (often not more than a few hours), which further shortens the available time to coordinate emergency response measures.

This section describes how ReAFFIRM has been applied in this study. Table 2 lists the different components of the method and summarises their resolutions.

Table 1
Example of the impact summary at a particular time step during a FF event (02.11.2015 2212 UTC; corresponding to Fig. 4 left). At this time step, 76 municipalities show simulated impacts, of which the 5 most severely affected are listed here.

	Simulated impacts		
Spatial Unit	Population in flooded area	Losses [k€]	Critical infrastr.
Catalonia (total)	989–3,145	31,505–69,449	3 Schools
Agramunt	666–818	10,426–14,063	2 Schools
Balaguer	0–1,136	3–5,011	
Tàrrega	121–397	2,434–6,351	
La Pobla de Cl.	71–157	2,079–4,005	
Camarasa	75–102	4,991–5,686	

3.1. Rainfall data and setup of the ERICHA system

The observations of the Creu del Vent radar (CDV; indicated in Fig. 6b) have been used in this study. CDV is a single-polarisation, C-Band Doppler radar operated by the Meteorological Service of Catalonia (SMC).

A chain of QPE algorithms (for details see Berenguer et al., 2015; Corral et al., 2009) has been applied to reduce effects of beam blockage, eliminate ground clutter and convert radar measurements into surface rainfall estimates. By comparison with rain gauges (of the SMC network), a uniform adjustment factor has been estimated for each individual rainfall event to compensate for systematic radar underestimation. This has been done to reduce the uncertainty in the rainfall inputs (i.e. the major forcing of the method), since it is not the goal of this paper to replicate operational conditions, but to focus on the translation from FF hazard into impacts. The resulting radar QPE accumulations have a resolution of 1 km and 6 min; this time step has been adopted for the execution of the ReAFFIRM runs.

The current version of the ERICHA system implemented in Catalonia uses a drainage network resolution of 200 m. The computation of the exceeded return period values T = [0, 2, 5, 10, 25, 50, 100, 200, 500] years is based on the analysis of long-term raingauge records (Ministerio de Fomento, 1999) and done in the cells with an upstream drainage area between 4 and 2000 km^2. The catchment concentration times have been estimated using the Témez (1978) formula.

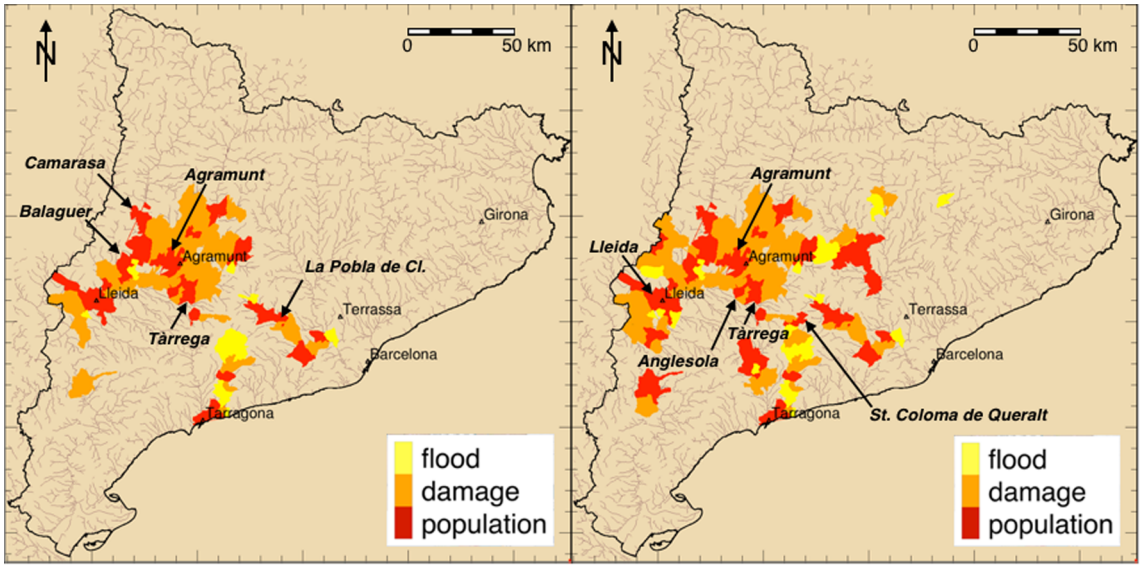

Fig. 4. Left: Simulated impact summary map at the municipality level of Catalonia at a specific time step during the event (02 November 2015 2212 UTC; corresponding to Table 1 and Fig. 3). Right: Impact summary map at the municipality level of Catalonia for the overall event (02–03 November 2015; corresponding to Table 3). Each municipality is coloured according to the upper bound of impacts (safe side) and the colours stand for: flooding of areas without significant risk (yellow), flood causing economic losses, but only in unpopulated areas (orange), and flooding of populated areas, which also implies the occurrence of economic losses (red). (For interpretation of the references to colour in this figure legend, the reader is referred to the web version of this article.)

3.2. Flood maps catalogue

We have used the flood maps generated in the framework of the EU Floods Directive by the two catchment authorities with responsibility in Catalonia (i.e. the Catalan Water Agency and the Ebro Hydrographic Confederation). Their simulations (ACA, 2013; MAPAMA, 2013) are available for the return periods T = [10, 50, 100, 500] years and have been combined to create a catalogue of flood maps that covers the entire region.

Flood depth data in Catalonia is publicly accessible in only a few river reaches, and not always reliable. Therefore, the flood maps catalogue has been created from the flood extent maps and we have assumed a uniform flood depth of 0.5 m in the flood cells for all return periods (as described in Section 2.2). A grid resolution of 25 m has been selected to depict the flood extent, as a compromise between sufficiently accurate representation and computation times that are suitable for real-time application (i.e. in the range of few minutes).

3.3. Socio-economic exposure and vulnerability data

The population density map has been created by combining three sources: In Catalonia, the map of Batista e Silva et al. (2013; reference year 2012; resolution 100 m) appears to be a good estimate for urban areas. In rural areas, it has minor gaps that were filled with values from Gallego (2010). Finally, the Corine Land Cover (CLC2012; see EEA, 2013) has been applied to filter for population density values in inhabited land uses (residential, industrial, and commercial).

The base for the economic loss estimation is also CLC2012, which has been reclassified into the seven land use classes proposed by Huizinga et al. (2017). For each land use class and each country in the world, Huizinga et al. (2017) developed a depth-damage curve to estimate the direct material losses. In this study, the curves for Spain have been selected without adjusting for economic inflation (Fig. 5).

For the estimation of affected critical infrastructures, a regional database has been employed. This database is currently under development within a cooperation between the Catalan Water Agency and the Catalan Civil Protection. Currently, the database includes schools and hospitals.

4. Results

ReAFFIRM has been tested for a number of FF events that occurred in Catalonia in the last 10 years. Out of those, three selected events are presented here to illustrate the capacities and limitations of the proposed approach. The three events affected different catchment types and showed differences in rainfall types, magnitudes, and temporal and spatial scales. Fig. 6 shows the overall rainfall accumulations of the events.

One of the challenges of the analysis of the results is the lack of systematic and quantitative impact information that can be used for validation. The only available source of this kind is a record of flood insurance claim data provided by the Consorcio de Compensación de Seguros (CCS, 2019). This database summarises direct losses from all kinds of flooding, also from flood types that ReAFFIRM naturally cannot detect (e.g. pluvial flooding, which often coincides in time with FFs). Furthermore, only insured and actually claimed (residential, commercial, and industrial) losses are included in their records (as a reference, the flood insurance penetration rate of private homes in Catalonia is

Table 2
Spatial, temporal, and return period resolutions of the ReAFFIRM components in Catalonia.

Component	Spatial resolution	Temporal resolution	Return period resolution [years]
Radar rainfall	1000 *m*	6 min	n/a
FF Hazard	200 *m*	6 min	T = [0, 2, 5, 10, 25, 50, 100, 200, 500]
Flood maps	25 *m*	6 min	T = [10, 50, 100, 500]
Impact assessment	25 *m*	6 min	n/a
Impact summary	municipality level	6 min	n/a

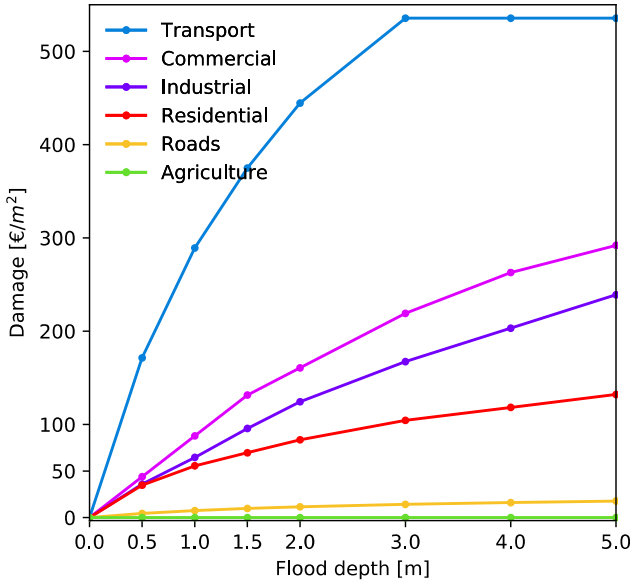

Fig. 5. Piecewise linear depth-damage curves (Huizinga et al., 2017; adjusted for Spain).

74.3%; UNESPA, 2017); losses related to public infrastructure or the agricultural sector are not included. In contrast, ReAFFIRM is designed to estimate the total direct losses. These fundamentally different characteristics of the simulation results and the available validation data impede a systematic and direct validation, e.g. by means of common indicators such as the probability of detection (POD) or the critical success index (CSI). Instead, the simulations have been evaluated qualitatively by comparing them with reported impacts after the event (mostly found in the media and social networks).

4.1. Event 1: Large-scale low-pressure front (2–3 November 2015)[1]

On the 02–03 November 2015, a large-scale low-pressure front crossed Catalonia from SW to NE[2] and brought rainfall accumulations of up to 200 mm in 24 h (Fig. 6a) that caused FFs and pluvial floods in several locations. CCS (2019) reported insured economic losses in 112 municipalities, of which the municipality of Agramunt (Lleida) was the most affected. Apart from significant economic losses mainly in the centre of Agramunt, two schools and one elderly home were flooded during the night. In contrast to the empty schools, people were sleeping in the basement of the elderly home. The warning reached the facility on the 03 November at 0303 UTC, when the Sió River had already started to flood the town. The basement could not be evacuated in time and four people died (Síndic, 2015).

4.1.1. Performance of the ERICHA system

In Agramunt, the basin of the Sió River has an area of 310 km^2 (see Fig. 2a and 6a) and is relatively flat. The estimated (Témez) concentration time is 12 h. The simulated return period at this location surpassed T = 10 years at 1942 UTC (02 November; see Fig. 2), more than seven hours before the onset of the flood, and remained above this threshold until 0248 UTC (03 November). Over the entire event, the maximum return period simulated at Agramunt exceeded 25 years. A few small streams in rural areas to the west of the city of Lleida show return periods over 100 years (not shown), however no significant impacts were reported from these specific locations.

[1] Note that the examples provided in section 2 (i.e. Table 1 and Figs. 2–4) correspond to this event.

[2] Animation of the rainfall field: http://crahi.upc.edu/ritter/reaffirm/event1_nov2015.gif.

4.1.2. Performance of the flood maps module

In Agramunt, the simulated flood extent has been compared to a map of geo-referenced flood observations from post-event newspaper articles and social-media postings[3], and 100% of the observed flood points are within the simulated flood extent (Fig. 3). This suggests that the combination of the ERICHA system and the flood map module performed well in this location.

4.1.3. Performance of the impact assessment module

The summary of impacts simulated by ReAFFIRM over the entire region and for the overall event is presented in Table 3 and the right panel of Fig. 4 (i.e. in each location, the highest impact of all time steps is displayed). ReAFFIRM identified widespread impacts throughout Catalonia, especially in the central part of the region. In total, impacts were simulated in 107 municipalities, of which the municipality of Agramunt shows the strongest signal in all three impact categories.

To introduce a more quantitative and systematic perspective into the validation, we have manually analysed the results across the region in the 37 municipalities with at least 25 k€ claimed losses (CCS, 2019) or 1 M€ simulated losses (upper bound) for this event. Summarising the results of this subjective analysis by municipalities allowed us to identify 13 hits (i.e. municipalities affected by floods, where ReAFFIRM estimated economic losses), 10 misses, and 14 false alarms. The reasoning behind these results and the underlying causes are presented in the Appendix.

In general, the simulated impact ranges between the lower and the upper bounds are very wide (there is often a factor of about 2 between the lower and the upper bounds of population in the flooded area or economic losses; see Table 3). This reflects a high degree of uncertainty. These wide ranges result from the coarse resolution of return periods in the flood maps catalogue (only four return periods are available; see Section 3.2 and Table 2).

Focusing again on Agramunt, the simulated range of 666–818 people in the flooded area seems realistic when comparing it to its overall population of 5,491 people (2015 census), and taking into account that a significantly large part of the town was flooded (about 15 – 20% of the urban area; see Fig. 3). CCS (2019) reported 1.1 M€ of insured private losses in the municipality. Additionally, the media mentioned that the damages on public infrastructures amounted to 0.4 M€[4], resulting in overall recorded losses of 1.5 M€. Confronting this value with the simulated losses of 10 – 14 M€ (Table 3) indicates that ReAFFIRM clearly overestimated the economic losses.

The two affected schools in Agramunt[5] were correctly identified to be flooded. Although the elderly home is also located in the simulated flooded area (Fig. 3), it was not explicitly captured by the impact assessment module, since the current infrastructure database includes only schools and hospitals (as mentioned in Section 3.3).

4.2. Event 2: Small-scale convective cells (24 September 2010)

In the afternoon of 24 September 2010, a few small convective cells developed in the coastal area around 50 km NE of Barcelona and remained stationary for around three hours[6]. The raingauge in Malgrat de Mar, a few km from the most affected area, accumulated 59 mm between 1500 UTC and 1900 UTC (Fig. 6b and Fig. 7). The affected catchments are very small (5 – 17 km^2) and steep and have short

[3] Sources: https://issuu.com/rbernaus/docs/sio621, https://www.youtube.com/watch?v=Yd4hGH-Mp7M.

[4] Source: https://lleidadiari.cat/provincia/agramunt-quantifica-en-421000-euros-els-danys-de-les-inundacions.

[5] Source: https://issuu.com/rbernaus/docs/sio621.

[6] Animation of the rainfall field: http://crahi.upc.edu/ritter/reaffirm/event2_sep2010.gif.

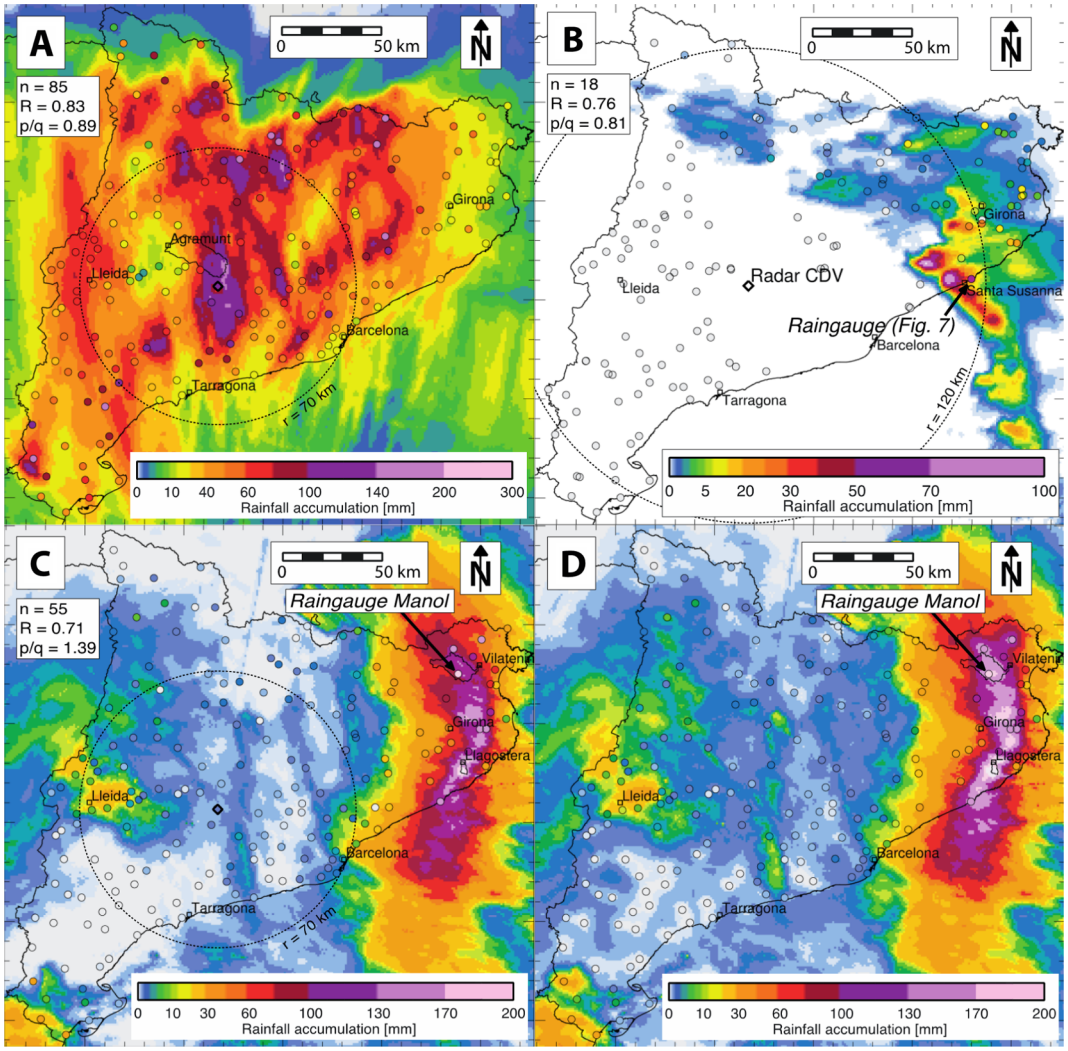

Fig. 6. Rainfall accumulations for the three events. Radar QPE and raingauges (circles) for (a) 02 November 2015 0600 UTC – 03 November 2015 0600 UTC, (b) 24 September 2010 1400–2000 UTC, and (c) 17 November 2018 1600 UTC – 18 November 2018 1600 UTC. For comparison between the accumulations in the raingauges and the corresponding radar pixels, panels a-c show the Pearson correlation (R), the ratio of total accumulations in raingauges (p) and radar pixels (q), and the number of raingauges (n) included in the analysis inside the indicated radar range (r). d) radar-raingauge-blending and raingauges (circles) for the same time span as in panel c.

Table 3
Summary of simulated and reported impacts (02.11. − 03.11.2015; corresponding to Fig. 4 right). In total, 107 municipalities show simulated impacts (only 5 listed here). Reported losses (CCS, 2019) include insured losses from all types of flooding (not only FFs).

Spatial Unit	ERICHA FF hazard [years]	Flooded area [ha]	Simulated impacts			Reported impacts	
			Population in flooded area	Losses [k€]	Critical infrastr.	Losses [k€]	Other
Catalonia (total)		5,879–9,911	1,411–5,442	62,032–131,529	4 Schools	2,730	
Agramunt	25	181–210	666–818	10,426–14,063;	2 Schools	1,059 (+421 in public losses)	4 casualties; 1 Elderly home; 2 Schools
Tàrrega	25	89–199	152–397	2,893–6,352		108 (+220 in public losses)	
Lleida	100	136–201	23–170	3,387–6,870		41 (+500 in public losses in overall province)	
Anglesola	10	424–735	2–6	2,068–3,724		72	
St. Coloma de Queralt	5	0–2	0–3	0–131		113	

concentration times in the range of 1 – 3 h. Their upper parts are mainly forested and they are highly urbanised near the coast, where the main impacts occurred. CCS (2019) reported insured private losses of 781,000 €, with the municipalities of Santa Susanna, Pineda de Mar, and Calella being the most significantly affected. The national road N-II had to be closed for some hours and several campsites were evacuated,

as reported by regional newspapers[7]. In total, the civil protection received 35 emergency calls in the area, mainly due to inundated homes and cars trapped in flooded roads.

The ERICHA system identified significant FF hazards in four locations (Fig. 8):

- Santa Susanna was the most severely affected municipality during the event, according to the reported impacts (Table 4). However, the FF hazard estimated by the ERICHA system in the Riera de Santa Susanna exceeded only T = 2 years. This indicates a hazard underestimation in this location. The apparent reason is that the radar did not fully capture the high rainfall intensities in the small catchment, due to the far distance from the radar and probably path attenuation of the signal by the high rainfall intensities (Fig. 6b). For reference, the radar QPE has been compared to the record of the nearest raingauge in Malgrat de Mar, around 3 km NE of Santa Susanna (see the location of the raingauge in Fig. 8). While the radar estimated a total accumulation of 27 mm at this location, the collocated raingauge measured 59 mm (Fig. 7). This significant rainfall underestimation is responsible for the low return period (T = 2 years) simulated in Santa Susanna.

Since the estimated hazard did not reach T = 5 years, no flood extent was simulated and thus ReAFFIRM did not identify any impacts in this location. Imposing a return period of 5 years in the Riera de Santa Susanna (which corresponds better to the observed impacts), results in very significant simulated impacts (values marked with * in Table 4).

- In Calella, the hazard estimated by the ERICHA system is T = 5 years (which qualitatively seems to correspond to the reported impacts; see Table 4). However, no impacts were simulated because there are no flood maps available in this location. In Catalonia, such gaps in the flood maps catalogue often appear in areas with low socio-economic flood exposure. However, occasionally the gaps also affect small streams that can be significant for flood risk management, such as in this case the Riera de Calella with a catchment area of only 6 km^2.
- In the municipality of Sant Cebrià, the ERICHA system estimated a return period of T = 10 years in the Riera de Sant Andreu (Fig. 8). The area in the vicinity of this stream is very sparsely populated and impacts were neither reported after the event nor simulated by ReAFFIRM (no flood maps are available in this location).
- Towards the South, the Riera de Pineda shows return periods of 5 and 10 years (Fig. 8), which appears to be in line with the flood magnitude. ReAFFIRM translated this hazard into significant socio-economic impacts in Pineda de Mar, as reported in Table 4.

Compared to Pineda de Mar's overall population of 21,381 (2010 census), the simulated upper bound of 8,577 people in the flooded area appears to correspond to the share of the town that is covered by the upper flood bound (around 50% of the urban area; see Fig. 9). However, only 35 emergency phone calls were recorded in the area[7], which gives the impression that much less people were affected in reality.

- Similarly as in event 1, the simulated economic losses of 0.6–28.1 M € in Pineda de Mar are well above the insured losses of 0.1 M€ (Table 4). Significant losses were computed all across the upper flood bound (Fig. 9). It can be observed that the uncertainty in the land use information impedes a reliable representation of the spatial variability of losses within the flooded area. For instance, the campsites were partly classified as commercial land use, resulting in higher simulated economic losses per m^2 than in the correctly classified residential areas in the town centre (i.e. although the employed dataset in general seemed to capture the real land uses reasonably well, we have observed a few local errors).
- The flooding of the national road N-II was correctly identified (Fig. 9), although the exact location has not been confirmed. Also the two campsites that were evacuated are clearly within the simulated upper flood bound. No reports have been found on possible inundations of schools or hospitals.

4.3. Event 3: Stationary low-pressure system (17–18 November 2018)

In the fall of 2018, Catalonia was hit by a series of rainfall episodes. One particular event was the result of a stationary low-pressure system that affected the NE part of the region during 17–18 November[8]. Rainfall accumulations of up to 176 mm in 24 h caused several streams to overflow. The regional newspapers and the Civil Protection reported the most important impacts in two locations:

- In the municipality of Figueres: parts of the village of Vilatenim, the highway C-260, and large areas of agricultural lands were flooded by the Manol River. A total of 21 persons had to be evacuated from their flooded homes[9].
- In the town of Llagostera (around 50 km south of Figueres): the Riera de Gotarra overflowed and around 40 houses[10] and several roads were flooded. The Civil Protection reported 32 emergency calls, of which 47% occurred between 0600 and 0700 UTC (18 November). The catchment upstream of Llagostera is relatively small (15 km^2) and steep, which caused a very sudden onset of the flood.

4.3.1. Performance of the ERICHA system

The most severely affected areas during this event are located more than 100 km far from the radar, which resulted in a relatively poor postprocessed radar QPE in these locations (Fig. 6c). To make the result analysis of ReAFFIRM less dependent on the quality of the rainfall inputs, the QPE maps for this event have been created using the radar-raingauge-blending technique of Velasco-Forero et al. (2009), which imposes raingauge observations while benefitting from the ability of the radar to depict the variability of the rainfall field. The resulting total event accumulation is shown in Fig. 6d.

The simulated hazard in the Manol River is T = 2 years (Fig. 10a). However, the Manol inundated wide areas[11], which indicates an underestimation of the hazard in this location. As described in the introduction, the ERICHA system is purely rainfall-based, and initial conditions (e.g. the effects of soil moisture) are not considered. In medium-sized and moderately flat catchments such as the Manol upstream of Vilatenim (165 km^2), the initial conditions can play a crucial role in events of lower return periods (Corral et al., 2019; Guillot and Duband, 1967) such as the present one. For this event, the simulations of EFAS showed that, in terms of the Soil Moisture Anomaly (SMA), the catchment was "much wetter" to "highly wetter than normal" (Fig. 11). These circumstances favoured a high discharge in the Manol, although the triggering rainfall was not that exceptional for this particular area (the maximum in the catchment, captured by the raingauge indicated in Fig. 6c and 10a, measured 176 mm in 24 h). Since the simulated hazard remained below T = 5 years, no flood extent (and thus no impacts)

[7] Source: https://www.vilaweb.cat/noticia/3780162/20100924/laiguat-causa-problemes-selva-valles-oriental-maresme.html.

[8] Animation of the rainfall field: http://crahi.upc.edu/ritter/reaffirm/event3_nov2018.gif.

[9] Source: https://www.gerio.cat/noticia/406753/el-desbordament-del-riu-manol-a-vilatenim-inunda-habitatges-i-desallotgen-21-persones.

[10] Source: https://twitter.com/JuditHuerta/status/1064161517992583168.

[11] Source: https://www.ccma.cat/324/les-imatges-aeries-de-les-inundacions-a-figueres/noticia/2887624/

Table 4
Summary of simulated and reported impacts (24.09.2010). The simulated impacts in Santa Susanna (marked with *) are the result of imposing a hazard of T = 5 years in the Riera de Santa Susanna.

Spatial Unit	ERICHA FF hazard [years]	Flooded area [ha]	Simulated impacts			Reported impacts
			Population in flooded area	Losses [k€]	Critical infrastr.	Losses [k€]
Catalonia (total)		9–99	10–8,577	556–28,106	5 Schools; 1 Hospital	781
Santa Susanna	2; (5)*	none; (0–80)*	none; (0–350)*	none; (0–11,239)*	none; (2 Schools)*	483
Pineda de Mar	5–10	8–98	11–8,577	556–28,106	5 Schools; 1 Hospital	107
Calella	5	none	none	none	none	31
St. Cebrià de Vallalta	10	1–1	0–0	0–0	none	0

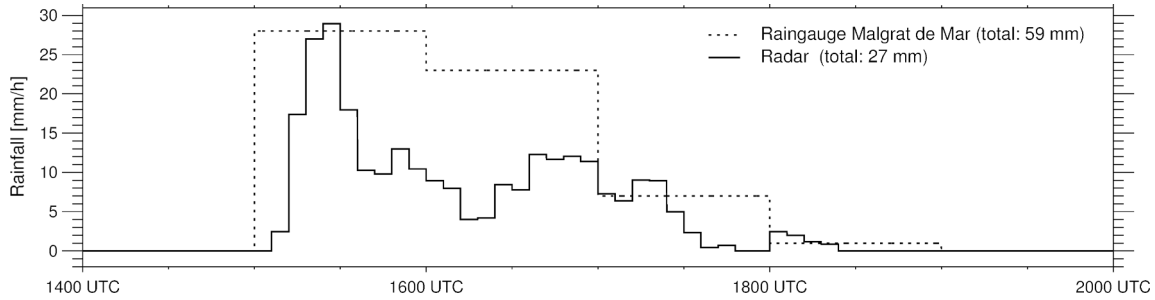

Fig. 7. Radar QPE (time resolution: 6 min) and raingauge rainfall (recorded every 60 min) intensities at Malgrat de Mar (24.09.2010).

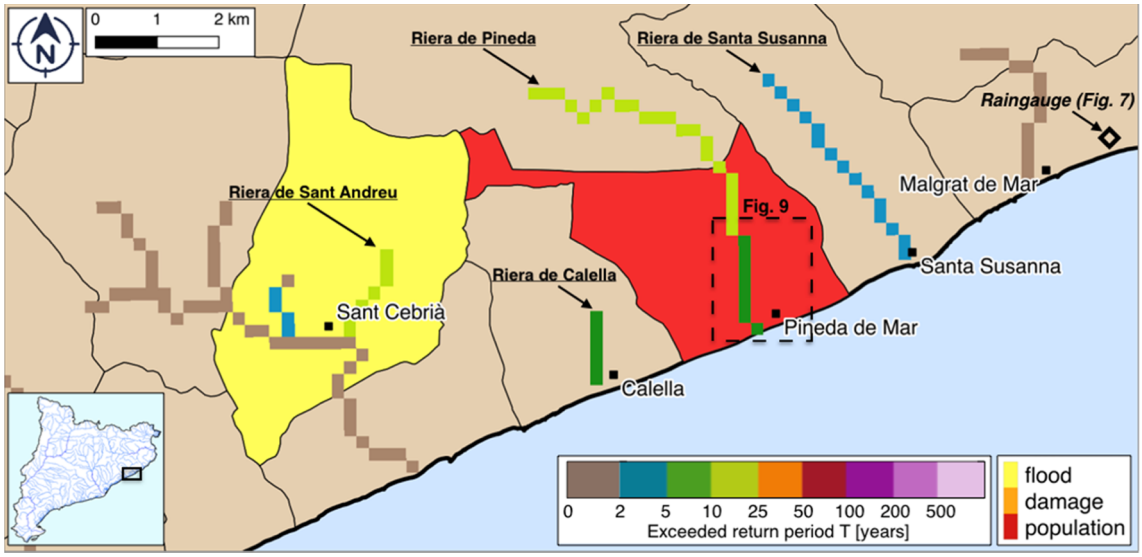

Fig. 8. ERICHA FF hazard in the drainage network and impact summary map at the municipality level for the overall event (24.09.2010 1400–2000 UTC). The dashed rectangle in Pineda de Mar indicates the domain displayed in Fig. 9.

were simulated in this location.

The simulated hazard in Llagostera reached its maximum of T = 5 years (Fig. 10b) at 0300 UTC, about 3 h ahead of the peak of the emergency calls recorded in this municipality.

4.3.2. Performance of the flood maps module

The flood extent at Llagostera was underestimated, as shown in Fig. 10c: All of the reported inundations are well outside the simulated upper flood bound, and some are even outside the original flood map of T = 100 years. This example illustrates a major limitation of ReAFFIRM: The flood maps in the catalogue account only for inundations that originate from the stream channel. However, in reality, FFs often coincide with pluvial flooding, which occurs when the rain rate exceeds the infiltration capacity of the soil or the capacity of the sewerage system. This combination of two flood types was likely the case during this event, since the flood observations[12] show both, the overflowing stream and the accumulated non-moving water that is typically observed during pluvial floods. In such combined events, ReAFFIRM covers only the part of the inundation that is caused by the overflow of the stream.

[12] Source: e.g. http://www.elpolltv.cat/index.php?option=com_k2&view=item&id=5994:desborda-la-riera-gotarra-al-seu-pas-per-llagostera&Itemid=673

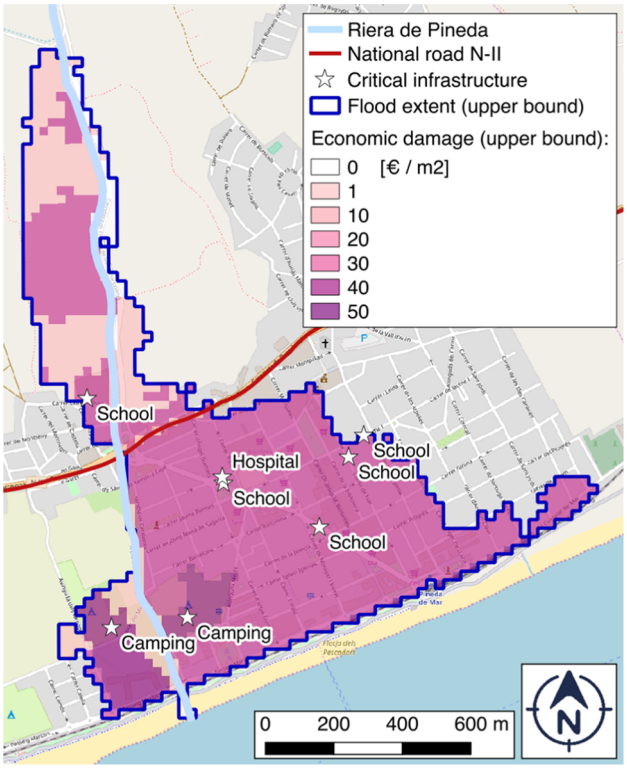

Fig. 9. Simulated flood extent (upper bound) and the corresponding economic losses in Pineda de Mar (24.09.2010). See Fig. 8 for the location of this domain within the affected part of the region.

4.3.3. Performance of the impact assessment module

The coexistence with pluvial flooding not considered by ReAFFIRM resulted in an underestimation of the impacts: The simulated impacts of 0 – 2 people and 0–30,000 € in economic losses in Llagostera are certainly too low (Table 5). When simulating the impacts using the flood maps for return periods of 50 and 100 years (which corresponds better to the observed flood extent; see Fig. 10c), ReAFFIRM estimates 110–220 people in the flooded area (marked with * in Table 5). This seems reasonable given the reported 32 emergency calls and 40 inundated houses described above. In contrast, the estimated economic losses of 1.3–3.2 M€ again appear to be very high, compared to the 0.2 M€ of insured losses (Table 5). This substantiates the systematic overestimation of economic losses found in the first two events.

As can be seen in Fig. 10a (see also Table 5), some less significant impacts were also detected along the Daró River, where the estimated return period exceeded T = 5 years in the municipalities of Gualta and Fontanilles. This is in line with the documented road closures and minor inundations in these two municipalities and in the surrounding areas along the Daró[13].

4.4. Comprehensive discussion

The previously presented results illustrate some of the capabilities and limitations of ReAFFIRM. It has been shown that the different components of the method are subject to numerous sources of uncertainty. In this subsection, some of the effects of these uncertainties on the accuracy of the impact estimates are summarised.

[13] Source: e.g. https://www.diaridegirona.cat/multimedia/videos/comarques/el-baix-emporda/2018–11-18–157733-daro-desbordant-passallis-llavia.html.

4.4.1. Performance of the ERICHA system

The radar QPE depicts the space–time variability of the rainfall field with resolutions appropriate for FF monitoring. We have seen, though, that the QPE accuracy has a direct effect on the quality of the ERICHA hazard assessments (e.g. in event 2, the flooding in Santa Susana was missed due to rainfall underestimation). In this study, uniform correction factors have been applied a posteriori to the QPE to compensate for systematic radar underestimation, which would not be possible in an operational setting. The QPE quality can also be improved by blending the radar rainfall with raingauge measurements (as done in event 3). This method is applied in real time in Catalonia for certain applications (e.g. Corral et al., 2009), but it is affected by the availability of raingauge observations (in real time, raingauge data become available only with certain time delays, in the range of minutes to hours). In an operational setting, the quality of the QPE would therefore be lower than in this study, introducing additional uncertainty into the FF hazard and impact estimation.

In the most severely affected areas (e.g. the town of Agramunt in event 1), the ERICHA system appeared to deliver reliable FF hazard assessments. The system is purely rainfall-based, which implies that initial catchment conditions such as soil moisture are neglected. During extreme events (as a reference, those with return periods exceeding 10 years), this simplification is assumed to have a secondary effect on the performance of the hazard estimation, but in events of lower return periods, the role of the catchment conditions can become more relevant (e.g. in event 3, the flooding of the Manol River was missed due to high antecedent wetness of the catchment).

4.4.2. Performance of the flood maps module

The flood maps catalogue in Catalonia covers only a small number (4) of return periods (see Table 2). Flood maps with return periods below 10 years were not available, and smaller events (e.g. with return periods below 5 years) could not be translated into impacts. The low resolution of return periods in the flood maps catalogue was also responsible for the wide uncertainty bands in the impact estimates (e.g. in many municipalities in event 1, there was a factor greater than 2 between the lower and the upper bounds of affected population and economic losses; see Table 3). Lastly, in the case study region, the EU Floods Directive maps were not always reliable and occasionally did not include streams that are small but potentially represent a risk (e.g. in event 2, the flooding in Calella was missed due to the lack of flood maps for the affected stream). The accuracy and comprehensiveness of the flood maps are crucial for the performance of the method, and the review of the flood risks in the ongoing second cycle of the EU Floods Directive is expected to improve their quality.

4.4.3. Performance of the impact assessment module

The performance of the translation from flood extents and depths into socio-economic impacts depends highly on the quality of the employed exposure and vulnerability datasets. The assessments of population in the flooded area and affected critical infrastructures seem to perform reasonably well. In contrast, the economic loss estimation suffers from high uncertainty, as it uses a combination of several data sources – some of them highly uncertain due to their empirical nature. Land use maps and especially depth-damage curves are inherently subject to high uncertainty (Merz et al., 2007). For instance, De Moel and Aerts (2011) quantified the uncertainties in the different components of flood damage models. They found that the influence of uncertainties in the land use data are moderate (a factor of 1.2 on the final loss estimates). In contrast, employing different sets of depth-damage curves from three different sources resulted in a factor of up to 4 on the loss estimates. Similarly, in our study, the uncertainty in the land use information was limited, and the large uncertainty in the loss estimation could mainly be attributed to the depth-damage information: With an assumed uniform flood depth of 0.5 m, the economic losses were overestimated by a factor of up to 10 in locations where the flood extent

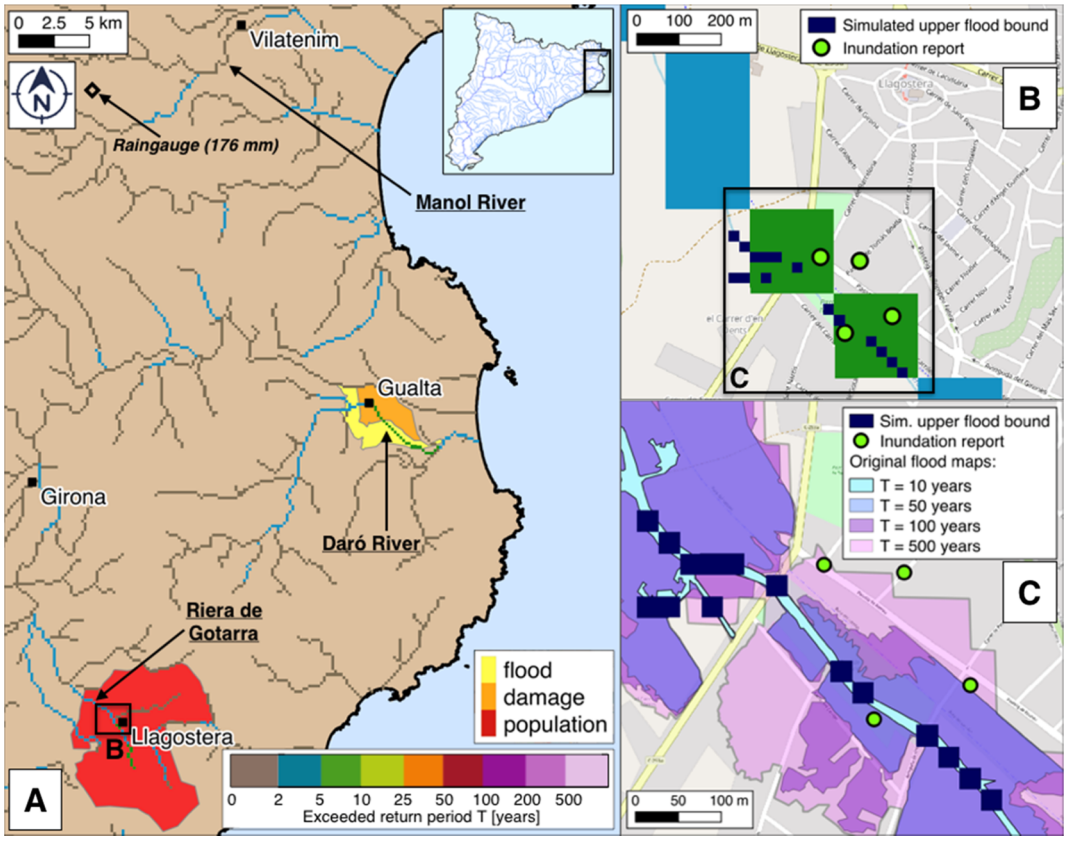

Fig. 10. (a) ERICHA FF hazard in the drainage network and impact summary map at the municipality level for the overall event (17.11. – 18.11.2018). (b) ERICHA FF hazard (in 200 m resolution cells) and corresponding high-resolution flood extent (upper bound) in Llagostera. c) Observed (Source: e.g. https://twitter.com/marc_elpoll/status/1064116450368135169) and simulated flood extent (upper bound), and original flood maps (of the EU Floods Directive) in Llagostera.

was simulated well (e.g. in event 1 in Agramunt). The employed depth-damage curves are linear for flood depths below 0.5 m (see Fig. 5). This means that, even when assuming lower flood depths, the large systematic overestimation of losses persists (e.g. an assumed flood depth of only 0.25 m would result in a loss overestimation by a factor of up to 5). This suggests that the systematic overestimation of losses originates from the uncertainty in the depth-damage curves. It is worth mentioning that Dottori et al. (2017) also used depth-damage curves from Huizinga et al. (2017) for estimating the impacts of large-scale river flooding in the Balkans. They also found high uncertainty in the loss estimates, but no systematic overestimation. One explanation for the systematic overestimation of losses in our study is that the depth-damage curves were created for large riverine floods that last a few days (Huizinga et al., 2017), whereas FFs typically last for only a few hours. Thieken et al. (2005) concluded that buildings that are flooded for less than 24 h suffer much fewer damages than those flooded for 2 days or more, while Kreibich et al. (2009) argued that the high flow velocities during FFs have usually only a small effect on the economic damages. Another factor that might contribute to the overestimation of losses are the relatively low return periods of the presented events, as people in the affected locations may have experienced floods of similar magnitudes in the past and adopted measures to reduce impacts.

5. Conclusions

This paper presents a method named ReAFFIRM that aims at enhancing the available information for emergency managers during flash floods, by complementing flash flood hazard estimates with components that automatically assess the expected socio-economic impacts at regional scale. It has been designed to have a moderate computational cost to facilitate real-time implementation.

ReAFFIRM consists of three main steps: First, the rainfall estimates are processed by the ERICHA system (Corral et al., 2019) that estimates the exceeded return period along a gridded drainage network with regional coverage. Then, the return periods are converted into high-resolution flood extents and depths, by applying a static catalogue of flood maps created in the context of the EU Floods Directive (European Commission, 2007). Finally, the flood depths are automatically combined with socio-economic exposure and vulnerability information to assess the flash flood impacts in three categories: population in the flooded area, economic losses, and affected critical infrastructures.

The method has been applied in the region of Catalonia (NE Spain). The results obtained in three events show that ReAFFIRM correctly identified the locations of the most significant impacts (e.g. where casualties occurred). However, some locations with less severe impacts were missed. In locations where the flood extent was estimated well, the assessments of population in the flooded area and affected critical infrastructures corresponded to the observed impacts. Conversely, an accurate estimation of economic losses at regional scale is currently not attainable (at least given the available models and data). However, the presented results seem to suggest that the relative magnitudes of the estimated losses over the region can help to identify the areas that suffer the highest damages, although more evidence is needed.

In general, ReAFFIRM's performance is highly dependent on the

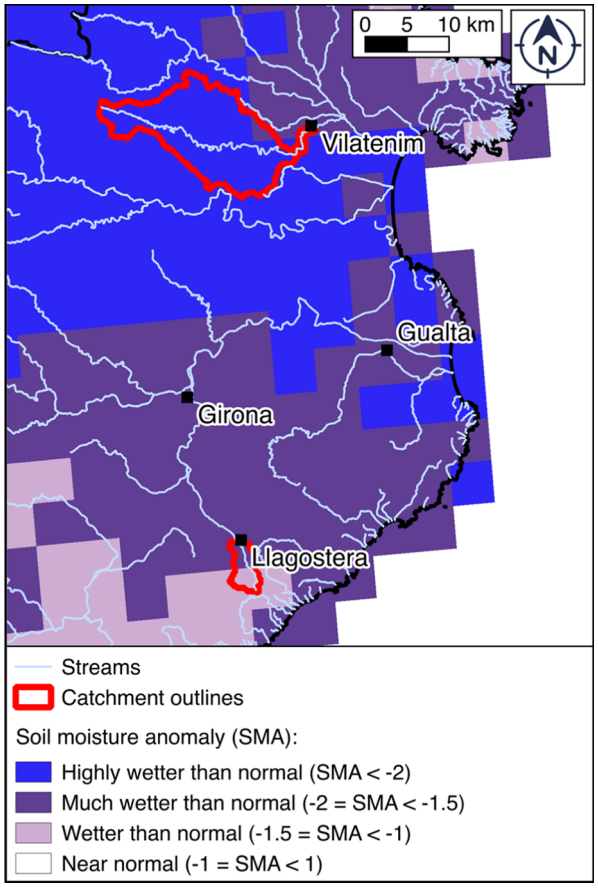

Fig. 11. Soil moisture anomaly (SMA) on 16 November 2018 (i.e. 1 day before the event). Data source: EFAS. The two red contours represent the catchment limits of the Manol River upstream of Vilatenim and the Riera de Gotarra upstream of Llagostera.

quality of the employed datasets: The key sources of uncertainty include (but are not limited to) the quality of the QPE, the comprehensiveness of the flood maps catalogue, and the accuracy of the depth-damage information. Methodological aspects, such as the purely rainfall-based flash flood hazard estimation, introduce additional uncertainties.

The added value of complementing the ERICHA flash flood hazard system with the impact assessment components has been demonstrated: Using only the ERICHA system as decision support, emergency managers would likely not prioritise in their decisions the locations with the highest potential impacts, but the locations showing the highest return periods in the stream network. For instance, in event 1, the most severely affected municipality (Agramunt) has been identified by ReAFFIRM as the one with the highest impacts, although the return period in this location was significantly lower than in other parts of the region.

The validation of impact estimates is not straightforward, since post-event observations of flash floods are often qualitative, biased or incomplete. For instance, in all three presented events, there were no stream gauges or flood extent surveys available in the most affected locations. The database of economic losses used for validation in this paper (CCS, 2019) captures only private insured losses, and it does not distinguish between flood types (e.g. losses from pluvial flooding add noise to the data). Newspaper articles and social media postings contain useful information (e.g. for verifying the exact locations of the impacts), but they are scattered and often do not report the full range of occurred impacts. Recently, we have started to use additional validation sources, such as real-time emergency phone calls and crowdsourcing data to test ReAFFIRM in a continuous setting (Ritter et al., 2019).

By design, transferring ReAFFIRM to other regions should be possible. The ERICHA flash flood hazard system has been recently implemented in real time in Switzerland, Liguria (NW Italy), and the island of Corsica (France), which was done in the framework of the EU H2020 project ANYWHERE (Corral et al., 2019). For the application of ReAFFIRM, the required flood maps (generated by the implementation of the EU Floods Directive) and the exposure and vulnerability data are publicly available with European coverage (note that a European database of critical infrastructures can be requested from Marin-Herrera, 2015).

Finally, the use of ReAFFIRM for early warning would require adding the capability of forecasting the expected impacts, providing extra time to the emergency responders to make decisions. Complementing the radar rainfall observations with Quantitative Precipitation Forecast (from NWP models and/or radar-based nowcasting; see e.g. Berenguer et al., 2005; Liechti et al., 2013) would enable lead-times of up to a few hours in addition to the lag time of the

Table 5
Summary of simulated and reported impacts (17.11. − 18.11.2018). The simulated impacts in Llagostera (marked with *) are the result of imposing the flood maps of T = 50 and T = 100 years as lower and upper flood bounds, which corresponds better to the observed flood extent (see Fig. 10c).

Spatial Unit	ERICHA FF hazard [years]	Flooded area [ha]	Simulated impacts			Reported impacts		
			Population in flooded area	Losses [k€]	Crit. infr.	Losses [k€]	Emergency calls	Other
Catalonia (total)		0–7	0–2	0–411	none			
Figueres (Vilatenim)	2	none	none	none	none	1,370	38	21 people evacuated
Llagostera	5; (50)*	0–1 (202–264)*	0–2; (110–220)*	0–30; (1,328–3,158)*	none; (none)*	213	32	40 houses
Gualta	5	0–5	0–0	0–381	none	38	0	1 road
Fontanilles	5	0–1	0–0	0–0	none	4	0	0

catchment. The performance of the resulting ReAFFIRM impact forecasting capabilities will be investigated in future work.

Declaration of Competing Interest

The authors declare that they have no known competing financial interests or personal relationships that could have appeared to influence the work reported in this paper.

Acknowledgements

This study has been carried out in the framework of the H2020 project ANYWHERE (H2020-DRS-1-2015-700099). The authors extend their gratitude to the Meteorological Service of Catalonia (SMC), the Catalan Water Agency (ACA), the Ebro Hydrographic Confederation (CHE), the Catalan Civil Protection, the Consorcio de Compensación de Seguros (CCS), and to Calum Baugh and the European Flood Awareness System (EFAS) for kindly providing data.

Appendix A

The available flood impact records used in section 4 do not allow for a systematic quantitative validation of the impact assessments, which is why the results have been validated qualitatively in Sections 4.1–4.3. With the aim to include some more quantitative aspects into the validation, the results of the most severe event (Section 4.1) have been manually evaluated by comparison with the insurance claim records across the entire region (CCS, 2019).

For the overall event, insurance claims were filed in 112 municipalities, while ReAFFIRM simulated economic losses in 107 municipalities. To enable a manual validation, the municipalities have first been filtered for those with at least 25 k€ claimed losses or 1 M€ simulated losses (upper bound). This resulted in a list of 37 municipalities. The results in these municipalities have been analysed one-by-one to identify hits, misses and false alarms and their potential causes (Table S1).

In 13 of the 37 analysed municipalities, significant economic losses appear in both, the ReAFFIRM simulations and the insurance claims ("hits"). In 10 municipalities with significant insurance claims, ReAFFIRM did not identify any losses. These "misses" occurred for two reasons:

Table S1
Performance of the ReAFFIRM economic loss estimation in the municipalities for event 1 (Section 4.1), by comparison with the flood insurance claim database from Consorcio de Compensación de Seguros (CCS, 2019).

Performance	Potential cause	Municipalities	Totals	
Hits		Agramunt, St Coloma de Queralt, Tàrrega, Anglesola, Lleida, Aiguamúrcia, Tarragona, Cervera, St Margarida de Montbui, Igualada, Montgai, Preixens, Alfarràs	13	
Misses	No flood maps available	Almacelles, Alpicat, Castellfollit de Riubregos, Rosello	4	10
	Pluvial flooding	El Montmell, Vilabella, Reus, Molins de Rei, El Pla de St Maria, Sant Cugat	6	
False alarms	Dry catchment	**Along the Anoia River:** St Sadurní, La Pobla de Claramunt, Vilanova del Camí, Gelida, Subirats	5	14
	Upstream dam retention	**Along the Cardener River:** Súria, Manresa, St Joan de Vilatorrada, Callús, Castellgalí **Along the Segre River:** Balaguer, Camarasa **Along the Noguera Ribagorçana River:** Corbins, Ivars de Noguera	9	

- No flood maps available: In four of the affected municipalities, the ERICHA system estimated significant return periods in streams close to residential, commercial, or industrial areas (which are the sectors covered in the insurance claim database). However, ReAFFIRM did not translate these return periods into economic losses, due to the lack of flood maps in these locations.
- Pluvial flooding: Insurance claims in six municipalities have been attributed to pluvial flooding, which (by design) is not detected by ReAFFIRM. The criterion for the attribution to pluvial flooding was that the claimed losses occurred outside the 500-year flood extent. In locations where no flood maps are available, claims that occurred at a distance greater than 200 m from the closest stream have been assumed to be associated to pluvial flooding.

In 14 municipalities, ReAFFIRM estimated significant economic losses, although no insurance claims were recorded. These "false alarms" occurred for two reasons:

- Dry catchments: Along the Anoia River, ReAFFIRM produced false alarms in five municipalities. Before the event, the catchment was highly drier than normal (Fig. S1), which may have resulted in high initial rainfall losses that decreased the flood magnitude. Since the ERICHA system is rainfall-based and does not account for the initial conditions, it likely overestimated the return periods (exceeding $T = 10$ years) in this location.
- Upstream dam retention: False alarms were also generated downstream of dams in the rivers Cardener (5), Segre (2), and Noguera Ribagorçana (2) (see Fig. S1). The upstream dams may have disposed of buffer capacities to lower the hydrograph peaks during the event. This aspect is not taken into account in the hazard estimation by the ERICHA system, and might have resulted in overestimations of the return periods in the Cardener ($T = 10$ years), the Segre ($T = 5$ years), and the Noguera Ribagorçana (up to $T = 25$ years).

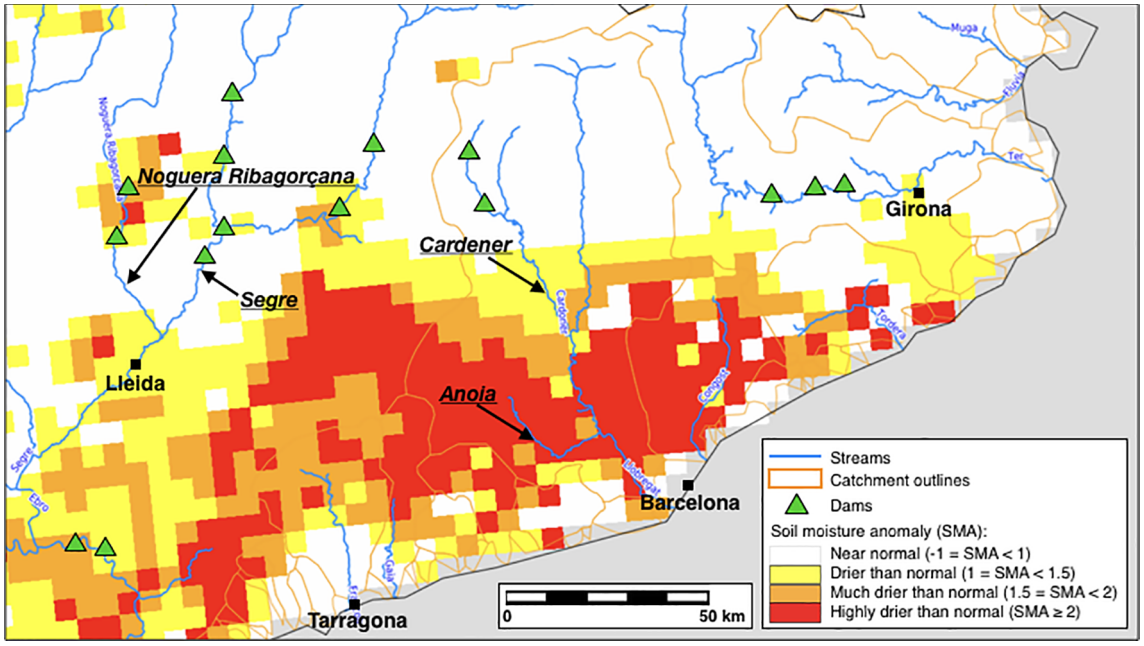

Fig. S1. Soil moisture anomaly (SMA) on 01 November 2015 (i.e. one day before the event). Data source: EFAS. The arrows indicate the rough locations of false alarms along the rivers Anoia, Cardener, Segre, and Noguera Ribagorçana.

Appendix B. Supplementary material

Supplementary data to this article can be found online at https://doi.org/10.1016/j.envint.2019.105375.

References

ACA, 2013. Agència Catalana de l'Aigua - Catàleg de descàrrega cartografia [www Document]. URL (accessed 9.13.18). [dataset]. http://aca.gencat.cat/ca/laigua/consulta-de-dades/descarrega-cartografica/.

Aldridge, T., Gunawan, O., Moore, R.J., Cole, S.J., Price, D., 2016. A surface water flooding impact library for flood risk assessment. E3S Web of Conferences 18006. https://doi.org/10.1051/e3sconf/20160718006.

Alfieri, L., Berenguer, M., Knechtl, V., Liechti, K., Sempere-Torres, D., Zappa, M., 2019. Flash Flood Forecasting Based on Rainfall Thresholds. In: Handbook of Hydrometeorological Ensemble Forecasting. Springer Berlin Heidelberg, Berlin, Heidelberg, pp. 1223–1260.

Alfieri, L., Salamon, P., Pappenberger, F., Wetterhall, F., Thielen, J., 2012. Operational early warning systems for water-related hazards in Europe. Environ. Sci. Policy 21, 35–49. https://doi.org/10.1016/j.envsci.2012.01.008.

Association of State Floodplain Managers, 2011. Critical Facilities and Flood Risk.

Batista e Silva, F., Gallego, J., Lavalle, C., 2013. A high-resolution population grid map for Europe. J. Maps 9, 16–28. https://doi.org/10.1080/17445647.2013.764830.

Berenguer, M., Corral, C., Sánchez-Diezma, R., Sempere-Torres, D., 2005. Hydrological Validation of a Radar-Based Nowcasting Technique. J. Hydrometeorol. 6, 532–549.

Berenguer, M., Sempere-Torres, D., Hürlimann, M., 2015. Debris-flow forecasting at regional scale by combining susceptibility mapping and radar rainfall. Hazards Earth Syst. Sci 15, 587–602. https://doi.org/10.5194/nhess-15-587-2015.

Berenguer, M., Sempere-Torres, D., Pegram, G.G.S., 2011. SBMcast - An ensemble nowcasting technique to assess the uncertainty in rainfall forecasts by Lagrangian extrapolation. J. Hydrol. 404, 226–240. https://doi.org/10.1016/j.jhydrol.2011.04.033.

Berenguer, M., Surcel, M., Zawadzki, I., Xue, M., Kong, F., 2012. The diurnal cycle of precipitation from continental radar mosaics and numerical weather prediction models. Part II: intercomparison among numerical models and with nowcasting. Mon. Weather Rev. 140, 2689–2705. https://doi.org/10.1175/MWR-D-11-00181.1.

Berne, A., Krajewski, W.F., 2013. Radar for hydrology: unfulfilled promise or unrecognized potential? Adv. Water Resour. 51, 357–366.

Blöschl, G., Reszler, C., Komma, J., 2008. A spatially distributed flash flood forecasting model. Environ. Model. Softw. 23, 464–478. https://doi.org/10.1016/j.envsoft.2007.06.010.

Borga, M., Boscolo, P., Zanon, F., Sangati, M., 2007. Hydrometeorological Analysis of the 29 August 2003 Flash Flood in the Eastern Italian Alps. J. Hydrometeorol. 8 (5), 1049–1067. https://doi.org/10.1175/JHM593.1.

Calianno, M., Ruin, I., Gourley, J.J., 2013. Supplementing flash flood reports with impact classifications. J. Hydrol. 477, 1–16. https://doi.org/10.1016/j.jhydrol.2012.09.036.

CCS, 2019. Base de datos. Daños asegurados por inundación (2000-2018). Madrid.

Clark, R.A., Gourley, J.J., Flamig, Z.L., Hong, Y., Clark, E., 2014. CONUS-Wide evaluation of national weather service flash flood guidance products. Weather Forecast. 29, 377–392. https://doi.org/10.1175/WAF-D-12-00124.1.

Cole, S.J., Moore, R.J., Wells, S.C., Mattingley, P.S., 2016. Real-time forecasts of flood hazard and impact: some UK experiences. In: E3S Web of Conferences, pp. 18015.

Corral, C., Berenguer, M., Sempere-Torres, D., Poletti, L., Silvestro, F., Rebora, N., 2019. Comparison of two early warning systems for regional flash flood hazard forecasting. J. Hydrol. 572, 603–619. https://doi.org/10.1016/j.jhydrol.2019.03.026.

Corral, C., Velasco, D., Forcadell, D., Sempere-Torres, D., Velasco, E., 2009. Advances in radar-based flood warning systems. The EHIMI system and the experience in the Besòs flash-flood pilot basin. Flood Risk Manage. Res. Pract. 309.

CRED, 2016. Annual disaster statistical review 2016: The numbers and trends. https://doi.org/10.1093/rof/rfs003.

de Moel, H., Aerts, J.C.J.H., 2011. Effect of uncertainty in land use, damage models and inundation depth on flood damage estimates. Nat. Hazards 58, 407–425. https://doi.org/10.1007/s11069-010-9675-6.

Dottori, F., Kalas, M., Salamon, P., Bianchi, A., Alfieri, L., Feyen, L., 2017. An operational procedure for rapid flood risk assessment in Europe. Nat. Hazards Earth Syst. Sci. 17, 1111–1126. https://doi.org/10.5194/nhess-17-1111-2017.

EEA, 2013. Copernicus Land Monitoring Service.

EEA, 2010. Mapping the impacts of recent natural disasters and technological accidents in Europe: an Overwiev of the last decade, EEA Environmental issue report – No. 35. https://doi.org/10.2800/62638.

European Commission, 2015. European Overview Assessment of Member States' reports on Preliminary Flood Risk Assessment and Identification of Areas of Potentially Significant Flood Risk. https://doi.org/10.2779/576456.

European Commission, 2007. DIRECTIVE 2007/60/EC OF THE EUROPEAN PARLIAMENT AND OF THE COUNCIL of 23 October 2007 on the assessment and management of flood risks, Official Journal of the European Union.

Faulkner, H., Parker, D., Green, C., Beven, K., 2007. Developing a translational discourse to communicate uncertainty in flood risk between science and the practitioner. AMBIO a J. Hum. Environ. 36, 692–704 10.1579/0044-7447(2007)36[692:DATDTC]2.0.CO;2.

Gallego, F.J., 2010. A population density grid of the European Union. Popul. Environ. 31, 460–473. https://doi.org/10.1007/s11111-010-0108-y.

Gaume, E., Bain, V., Bernardara, P., Newinger, O., Barbuc, M., Bateman, A., Blaškovičová, L., Blöschl, G., Borga, M., Dumitrescu, A., Daliakopoulos, I., Garcia, J., Irimescu, A., Kohnova, S., Koutroulis, A., Marchi, L., Matreata, S., Medina, V., Preciso, E., Sempere-Torres, D., Stancalie, G., Szolgay, J., Tsanis, I., Velasco, D., Viglione, A., 2009. A compilation of data on European flash floods. J. Hydrol. 367, 70–78. https://doi.org/10.1016/J.JHYDROL.2008.12.028.

Georgakakos, K.P., 2006. Analytical results for operational flash flood guidance. J. Hydrol. 317, 81–103. https://doi.org/10.1016/j.jhydrol.2005.05.009.

Georgakakos, K.P., 1986. On the design of national, real-time warning systems with capability for site-specific, flash-flood forecasts. Bull. Am. Meteorol. Soc. 67,

1233–1239. https://doi.org/10.1175/1520-0477(1986) 067<1233:OTDONR>2.0.CO;2.
Germann, U., Berenguer, M., Sempere-Torres, D., Zappa, M., 2009. REAL – Ensemble radar precipitation estimation for hydrology in a mountainous region. Q. J. R. Meteorol. Soc. 135, 445–456.
Gourley, J.J., Flamig, Z.L., Hong, Y., Howard, K.W., 2014. Evaluation of past, present and future tools for radar-based flash-flood prediction in the USA. Hydrol. Sci. J. 59, 1377–1389. https://doi.org/10.1080/02626667.2014.919391.
Grillakis, M.G., Koutroulis, A.G., Komma, J., Tsanis, I.K., Wagner, W., Blöschl, G., 2016. Initial soil moisture effects on flash flood generation - A comparison between basins of contrasting hydro-climatic conditions. J. Hydrol. 541, 206–217. https://doi.org/10.1016/j.jhydrol.2016.03.007.
Guillot, P., Duband, D., 1967. La méthode du GRADEX pour le calcul de la probabilité des crues à partir des pluies. In: Colloque International Sur Les Crues et Leur Évaluation. Leningrad, pp. 15–22.
Hapuarachchi, H.A.P., Wang, Q.J., Pagano, T.C., 2011. A review of advances in flash flood forecasting. Hydrol. Process. 25, 2771–2784. https://doi.org/10.1002/hyp.8040.
Huizinga, J., de Moel, H., Szewczyk, W., 2017. Global flood depth-damage functions: Methodology and the Database with Guidelines. https://doi.org/10.2760/16510.
Javelle, P., Demargne, J., Defrance, D., Pansu, J., Arnaud, P., 2014. Evaluating flash-flood warnings at ungauged locations using post-event surveys: a case study with the AIGA warning system. Hydrol. Sci. J. 59. https://doi.org/10.1080/02626667.2014.923970.
Javelle, P., Fouchier, C., Arnaud, P., Lavabre, J., 2010. Flash flood warning at ungauged locations using radar rainfall and antecedent soil moisture estimations. J. Hydrol. 394, 267–274. https://doi.org/10.1016/j.jhydrol.2010.03.032.
Jonkman, S.N., 2007. Loss of life estimation in flood risk assessment.
Kreibich, H., Piroth, K., Seifert, I., Maiwald, H., Kunert, U., Schwarz, J., Merz, B., Thieken, A.H., 2009. Is flow velocity a significant parameter in flood damage modelling? Hazards Earth Syst. Sci 9, 1679–1692.
Le Bihan, G., Payrastre, O., Gaume, E., Moncoulon, D., Pons, F., 2017. The challenge of forecasting impacts of flash floods: Test of a simplified hydraulic approach and validation based on insurance claim data. Hydrol. Earth Syst. Sci. 21, 5911–5928. https://doi.org/10.5194/hess-21-5911-2017.
Liechti, K., Panziera, L., Germann, U., Zappa, M., 2013. The potential of radar-based ensemble forecasts for flash-flood early warning in the southern Swiss Alps. Hydrol. Earth Syst. Sci 17, 3853–3869. https://doi.org/10.5194/hess-17-3853-2013.
MAPAMA, 2013. Ministerio de Agricultura y Pesca, Alimentación y Medio Ambiente - Zonas Inundables asociadas a periodos de retorno [WWW Document]. URL (accessed 9.13.18). [dataset]. http://www.mapama.gob.es/es/cartografia-y-sig/ide/descargas/agua/zi-lamina.aspx.
Marchi, L., Borga, M., Preciso, E., Gaume, E., 2010. Characterisation of selected extreme flash floods in Europe and implications for flood risk management. J. Hydrol. 394, 118–133. https://doi.org/10.1016/j.jhydrol.2010.07.017.
Marin-Herrera, M., Batista e Silva, F., Bianchi, A., Barranco, R., Lavalle, C., 2015. A geographical database of Infrastructures in Europe. https://doi.org/10.2788/22910.
Merz, B., Thieken, A.H., Gocht, M., 2007. Flood Risk Mapping At The Local Scale: Concepts and Challenges, in: Flood Risk Management in Europe. Springer Netherlands, Dordrecht, pp. 231–251. https://doi.org/10.1007/978-1-4020-4200-3_13.
Ministerio de Fomento, 1999. Máximas lluvias diarias en España Peninsular. [dataset].
Norbiato, D., Borga, M., Degli Esposti, S., Gaume, E., Anquetin, S., 2008. Flash flood warning based on rainfall thresholds and soil moisture conditions: An assessment for gauged and ungauged basins. J. Hydrol. 362, 274–290. https://doi.org/10.1016/j.jhydrol.2008.08.023.
Ntelekos, A.A., Georgakakos, K.P., Krajewski, W.F., 2006. On the uncertainties of flash flood guidance: toward probabilistic forecasting of flash floods. J. Hydrometeorol. 7, 896–915. https://doi.org/10.1175/JHM529.1.
Park, S., Berenguer, M., Sempere-Torres, D., 2019. Long-term analysis of gauge-adjusted radar rainfall accumulations at European scale. J. Hydrol. 573, 768–777.
Ramos, M.H., Van Andel, S.J., Pappenberger, F., 2013. Do probabilistic forecasts lead to better decisions? Hydrol. Earth Syst. Sci. 17, 2219–2232. https://doi.org/10.5194/hess-17-2219-2013.
Raynaud, D., Thielen, J., Salamon, P., Burek, P., Anquetin, S., Alfieri, L., 2015. A dynamic runoff co-efficient to improve flash flood early warning in Europe: Evaluation on the 2013 central European floods in Germany. Meteorol. Appl. 22, 410–418. https://doi.org/10.1002/met.1469.
Revilla-Romero, B., Shelton, K., Wood, E., Berry, R., Bevington, J., Lewis, G., Gubbin, A., Griffiths, S., Barnard, P., Pinnell, M., 2017. Flood Foresight : A near-real time flood monitoring and forecasting tool for rapid and predictive flood impact assessment. Geophys. Res. Abstracts 2017.
Ritter, J., Berenguer, M., Corral, C., Park, S., Sempere-Torres, D., 2019. Testing conventional and unconventional data sources for the validation of a real-time flash flood impact model. EGU General Assembly Conference Abstracts. pp. EGU2019-1330.
Saint-Martin, C., Fouchier, C., Javelle, P., Douvinet, J., Vinet, F., 2016. Assessing the exposure to floods to estimate the risk of flood-related damage in French Mediterranean basins. In: Assessing the exposure to floods to estimate the risk of flood-related damage in French Mediterranean basins. E3S Web of Conferences, pp. 04013 https://doi.org/10.1051/e3sconf/20160704013.
Schauwecker, S., Gascón, E., Park, S., Ruiz-Villanueva, V., Schwarb, M., Sempere-Torres, D., Stoffel, M., Vitolo, C., Rohrer, M., 2019. Anticipating cascading effects of extreme precipitation with pathway schemes - three case studies from Europe. Environ. Int. 127, 291–304.
Sene, K., 2013. Flash Floods. Springer. https://doi.org/10.1007/978-94-007-5164-4.
Silvestro, F., Rebora, N., 2011. Quantitative flood forecasting on small-and medium-sized basins: a probabilistic approach for operational purposes. J. Hydrometeorol. 12, 1423–1446. https://doi.org/10.1175/JHM-D-10-05022.1.
Silvestro, F., Rossi, L., Campo, L., Parodi, A., Fiori, E., Rudari, R., Ferraris, L., 2019. Impact-based flash-flood forecasting system: Sensitivity to high resolution numerical weather prediction systems and soil moisture. J. Hydrol. 572, 388–402. https://doi.org/10.1016/j.jhydrol.2019.02.055.
Síndic, 2015. Resolución del expediente AO-00185/2015, relativo a la muerte de cuatro personas mayores de la Residencia Ribera de Sió de Agramunt al desbordarse el rio Sió. Barcelona.
Spitalar, M., Gourley, J.J., Lutoff, C., Kirstetter, P.E., Brilly, M., Carr, N., 2014. Analysis of flash flood parameters and human impacts in the US from 2006 to 2012. J. Hydrol. 519, 863–870. https://doi.org/10.1016/j.jhydrol.2014.07.004.
Témez, J.R., 1978. Calculo hidrometeoorologico de caudales maximos en pequenas cuencas naturales. Madrid.
Thieken, A.H., Müller, M., Kreibich, H., Merz, B., 2005. Flood damage and influencing factors: New insights from the August 2002 flood in Germany. Water Resour. Res. 41. https://doi.org/10.1029/2005WR004177.
UNESPA, 2017. Informe Estamos Seguros. Madrid.
Velasco-Forero, C.A., Sempere-Torres, D., Cassiraga, E.F., Jaime Gómez-Hernández, J., 2009. A non-parametric automatic blending methodology to estimate rainfall fields from rain gauge and radar data. Adv. Water Resour. 32, 986–1002. https://doi.org/10.1016/j.advwatres.2008.10.004.
Vincendon, B., Édouard, S., Dewaele, H., Ducrocq, V., Lespinas, F., Delrieu, G., Anquetin, S., 2016. Modeling flash floods in southern France for road management purposes. J. Hydrol. 541, 190–205. https://doi.org/10.1016/j.jhydrol.2016.05.054.
WMO, 2015. WMO Guidelines on Multi-hazard Impact-based Forecast and. Warning Services.
WMO, 2008. Guidelines on communicating forecast uncertainty, Organization.
Wood, E.F., Sivapalan, M., Beven, K., 1990. Similarity and scale in catchment storm response. Rev. Geophys. https://doi.org/10.1029/RG028i001p00001.
Yatheendradas, S., Wagener, T., Gupta, H., Unkrich, C., Goodrich, D., Schaffner, M., Stewart, A., 2008. Understanding uncertainty in distributed flash flood forecasting for semiarid regions. Water Resour. Res. 44. https://doi.org/10.1029/2007WR005940.
Zappa, M., Beven, K.J., Bruen, M., Cofiño, A.S., Kok, K., Martin, E., Nurmi, P., Orfila, B., Roulin, E., Schröter, K., Seed, A., Szturc, J., Vehviläinen, B., Germann, U., Rossa, A., 2010. Propagation of uncertainty from observing systems and NWP into hydrological models: COST-731 working group 2. Atmos. Sci. Lett. 11, 83–91.